An experimental study of the mechanism and branching ratio for the reaction between methyl formate and chlorine atoms

ARTICLE *in* CHEMICAL PHYSICS LETTERS · OCTOBER 2002

Impact Factor: 1.9 · DOI: 10.1016/S0009-2614(02)01424-0

Available online at www.sciencedirect.com
SCIENCE DIRECT®
Chemical Physics Letters 365 (2002) 267–278
CHEMICAL PHYSICS LETTERS
www.elsevier.com/locate/cplett

An experimental study of the mechanism and branching ratio for the reaction between methyl formate and chlorine atoms

Jaron C. Hansen [a], Joseph S. Francisco [a,*], Joseph J. Szente [b], M. Matti Maricq [b,1]

[a] *Department of Chemistry and Department of Earth and Atmospheric Science, Purdue University, West Lafayette, IN 47907-1393, USA*
[b] *Research Laboratory, Ford Motor Company, P.O. Box 2053, Drop 3083, Dearborn, MI 48121, USA*

Received 19 April 2002; in final form 6 August 2002

Abstract

FTIR spectroscopy/UV laser flash photolysis has been used to examine the reaction of chlorine atoms with methyl formate ($CH_3OC(O)H$) at 296 K. The reaction has two possible branches; extraction of a methyl hydrogen or the carbonyl hydrogen. Measurements of the product yields indicate that abstraction of the carbonyl hydrogen is favored over the methyl hydrogen by $58 \pm 6\%$ ($k_{1a} = 8.1 \times 10^{-13}$ cm^3 mol^{-1} s^{-1}) to $42 \pm 6\%$ ($k_{1b} = 5.9 \times 10^{-13}$ cm^3 mol^{-1} s^{-1}). The experimentally determined IR spectrum of $CH_2ClOC(O)H$ and $CH_3OC(O)Cl$ are presented and verified with high level ab initio calculations.

1. Introduction

Concerns about mobile source emissions and their impact on tropospheric chemistry have spurred research into alternative fuels with the goal of reducing emissions of CO, NO_x, and particulate matter. Fuel composition affects the tendency of a fuel to form soot and NO_x. With this in mind, oxygenated hydrocarbons such as ethers can be added to fuels to maintain performance while lowering tailpipe emissions of CO [1]. Dimethyl ether (DME) is one such alternative fuel that has been proposed as a diesel fuel substitute. The atmospheric oxidation of DME has been studied by Japar et al. [2], Jenkin et al. [3], Wallington et al. [4], Langer et al. [5], Sehested et al. [6,7], and Maricq et al. [8]. Japar et al. [2] used Cl atom initiated hydrogen abstraction to simulate the reaction of DME with tropospheric OH radical in the presence of NO. Reaction products were determined using FTIR spectroscopy. The production of methyl formate ($CH_3OC(O)H$) accompanied the loss of dimethyl ether quantitatively. The yield of methyl formate relative to DME loss was found to be 0.902.

* Corresponding author. Fax: +1-765-494-0239.
E-mail address: jfrancis@purdue.edu (J.S. Francisco).
[1] Also Corresponding author.

0009-2614/02/$ - see front matter
PII: S0009-2614(02)01424-0

Since these results were published, a number of papers have appeared on the oxidation mechanism of methyl formate. Good et al. [9,10] in two papers studied both experimentally and computationally the kinetics and mechanism of the reaction between methyl formate and Cl as well as OH. In a separate work, Good et al. [11] used high level ab initio calculations in conjunction with transition state theory to predict the branching ratio for methyl formate for the reaction with chlorine atoms. They reported a 90% probability for extraction of the carbonyl hydrogen based on the calculated activation barrier and pre-exponential factor. Due to the small activation barriers calculated for the extraction of both the carbonyl or methyl hydrogens, 0.2 and 1.9 kcal mol^{-1}, respectively, the computational uncertainty of ± 0.5 kcal mol^{-1} leads to a calculated branching fraction for extraction of the carbonyl hydrogen that ranges from 65% to 97%.

Good et al. [11] compared their theoretical result to the experimentally determined branching ratio for the analogous reaction between chlorine atom and acetaldehyde ($CH_3C(O)H$). For the acetaldehyde system, the branching ratio was reported to be 92% extraction of the carbonyl hydrogen [12], which was consistent with the calculated value for the analogous chlorine atom reaction with methyl formate. The goal of this work is to experimentally determine the branching ratio for methyl formate when hydrogen extraction takes place by reaction with chlorine atoms. This information will allow evaluation of the previous ab initio branching ratio and consequently help provide a more complete understanding of the potential effects on the environment of the use of dimethyl ether as a fuel. In addition the experimentally determined IR spectra of $CH_2ClOC(O)H$ and $CH_3OC(O)Cl$ will be presented. High level ab initio calculations will be used to verify the IR spectra of $CH_2ClOC(O)H$ and $CH_3OC(O)Cl$.

The reaction between methyl formate and chlorine is expected to proceed according to the following series of reactions in the presence of excess Cl_2:

$$CH_3OC(O)H + Cl^{\cdot} \rightarrow CH_3OC^{\cdot}(O) + HCl \quad (1a)$$

$$CH_3OC(O)H + Cl^{\cdot} \rightarrow {}^{\cdot}CH_2OC(O)H + HCl \quad (1b)$$

$$CH_3OC^{\cdot}(O) + Cl_2 \rightarrow CH_3OC(O)Cl + Cl^{\cdot} \quad (2)$$

$$CH_3OC^{\cdot}(O) + Cl^{\cdot} \rightarrow CH_3OC(O)Cl \quad (3)$$

$${}^{\cdot}CH_2OC(O)H + Cl_2 \rightarrow CH_2ClOC(O)H + Cl^{\cdot} \quad (4)$$

$${}^{\cdot}CH_2OC(O)H + Cl^{\cdot} \rightarrow CH_2ClOC(O)H \quad (5)$$

al. [10] show large activation barriers for the unimolecular decomposition of $CH_3OC(O)$ and $CH_2OC(O)H$. As such it is not expected that the unimolecular decomposition will play a role in the loss of these radicals. The amount of $CH_3OC(O)Cl$ and $CH_2ClOC(O)H$ produced relative to the amount of $CH_3OC(O)H$ removed allows for determination of the branching ratio of reactions (1a) and (1b). The chain reaction will continue with the chlorinated compounds until all of the methyl formate has become fully chlorinated. These latter reactions do not play a significant role until most of the original methyl formate has reacted with chlorine atoms. The kinetics associated with reactions (1a), (1b), (2)–(5) dictate that until 50% of the methyl formate has been removed, multi-chlorinated methyl formate is expected to be less than 5% of the total yield.

2. Experimental method

2.1. Experimental method

The experimental apparatus consists of a 656 cm^3 square Teflon sample cell with a 16.1 cm long probe beam pathlength fitted with NaCl windows. Perpendicular to the probe beam path is a 19.7 cm long photolysis pathlength with quartz windows at the ends, allowing for passage of UV light. Depending on the choice of experimental conditions, the cell is filled with a combination of methyl formate (1–3 Torr) (Aldrich 99.9%), $CH_3OC(O)Cl$ (Aldrich, 99%), chlorine (20–25 Torr) (Scott Specialty Gases 99.9%), and high

purity helium (20–100 Torr) (BOC 99.9%). The reaction mixture is probed using a Matteson Instruments Galaxy 7020 series FTIR operating in the mid-IR with 1 cm^{-1} resolution. Each measured spectrum is comprised of 32 co-added and averaged individual spectra. Gas pressures are monitored using an MKS Baratron® capacitance manometer with ±0.1 Torr accuracy.

Hydrogen extraction by chlorine atom reaction is initiated by photolyzing a small amount of the chlorine with 351 nm light from a Lambda Physik Compex Model 102 excimer laser firing at 2 Hz with an average energy between 6.5–30 mJ $pulse^{-1}$. After the initial generation of chlorine atoms by UV photolysis, a chain reaction involving methyl formate radicals and molecular chlorine (Reactions (2) and (4)) results in the net removal of $(5–20)\times 10^{14}$ mol cm^{-3} of methyl formate after 10–20 laser shots.

Before each experimental run, an IR spectrum of the methyl formate and chlorine gas mixture is taken to quantify the methyl formate concentration as well as to verify the absence of other products. The reaction mixture is then photolyzed with 10–20 laser pulses, after which the IR spectrum is immediately re-measured. This process is repeated several times, stopping between each set of laser pulses to take an IR spectrum. After a total of 70–100 shots, approximately 10–30% of the methyl formate has reacted with the chlorine. In most cases, measurements are continued until the spectral features attributed to methyl formate indicate that at least 50% of the methyl formate has been removed. At this point, less than 5% of the mono-chlorinated methyl formate has reacted with chlorine. Only the spectra obtained within the first 0–70 laser pulses are analyzed to determine the branching ratio. This minimizes the influence of multiple chlorinated methyl formate species on the IR spectra.

Due to the design of the reaction cell, only 16% of the volume is irradiated by the photolysis beam. Some mixing due to diffusion will occur between each laser shot; however, it is estimated that complete mixing to reach a relatively homogeneous distribution requires 2–10 s depending on the total pressure. The depletion of chlorine and methyl formate following each laser shot is quite small relative to their initial concentrations, <1%. To demonstrate that the time delay between photolysis and probing does not have an effect, IR spectra were measured immediately at the conclusion of the photolysis pulses as well as 5, 10, and 15 min after the photolysis event. The IR intensities were found to vary by <1% between the four time delays indicating that the reactions are complete by the time the IR spectrum is measured and that mixing or wall losses do not affect the measurements.

2.2. Computational method

The GAUSSIAN 98 suite [13] of programs in conjunction with density functional theory (DFT) is used to verify the experimentally determined IR spectrum of a number of intermediate chlorinated methyl formate species. This was necessary because samples of $CH_2ClOC(O)H$ and $CH_2ClOC(O)Cl$ are unavailable commercially. The IR spectrum of $CH_3OC(O)Cl$ was calculated in order to serve as a calibrate for the unknown IR spectra of $CH_2ClOC(O)H$, and $CH_2ClOC(O)Cl$. Theoretical IR spectra for $CH_2ClOC(O)H$, $CH_2ClOC(O)Cl$ and $CH_3OC(O)Cl$ are produced by optimizing the geometry of each species using density functional theory coupled with a number of basis sets. Beck's three parameter with non-correlation and Lee–Yang–Parr full correlation (B3LYP) are used in conjunction with the 6-31G(d), 6-31G(d,p), 6-311++G(d,p), 6-311++G(2df,2p), and 6-311++G(3df,3pd) basis sets. The vibrational frequencies are calculated at a B3LYP/6-31G(d) level. Work by Scott et al. [14] shows a high degree of accuracy between experimental and computational IR spectra can be achieved by use of the B3LYP/6-31G(d) basis set and a scaling factor of 0.9614. A detailed explanation of the procedure used to generate the calculated IR spectrum has been given previously [15]. Briefly, a Lorenzian probability distribution, with a full-width-at-half-maximum of 16 cm^{-1} chosen to match the experimental line width, is fit around each calculated and scaled fundamental frequency.

3. Results

The removal of methyl formate in the presence of Cl_2 and Cl atoms as a function of total laser shots is given in Fig. 1. Prior to exposure to the UV laser pulses (laser shots = 0, i.e., time = 0), the IR spectrum shows that only methyl formate is present. As the mixture is irradiated by the first 40 laser shots, IR features attributed to methyl formate are removed and new features representing $CH_2ClOC(O)H$ and $CH_3OC(O)Cl$ become apparent. As the reaction mixture continues to be irradiated, eventually all of the methyl formate is removed and new features representing multiply-chlorinated methyl formate species become prominent. Only the IR spectra taken at early times (0–70 photolysis pulses) are analyzed for branching ratio information. This is done to minimize the

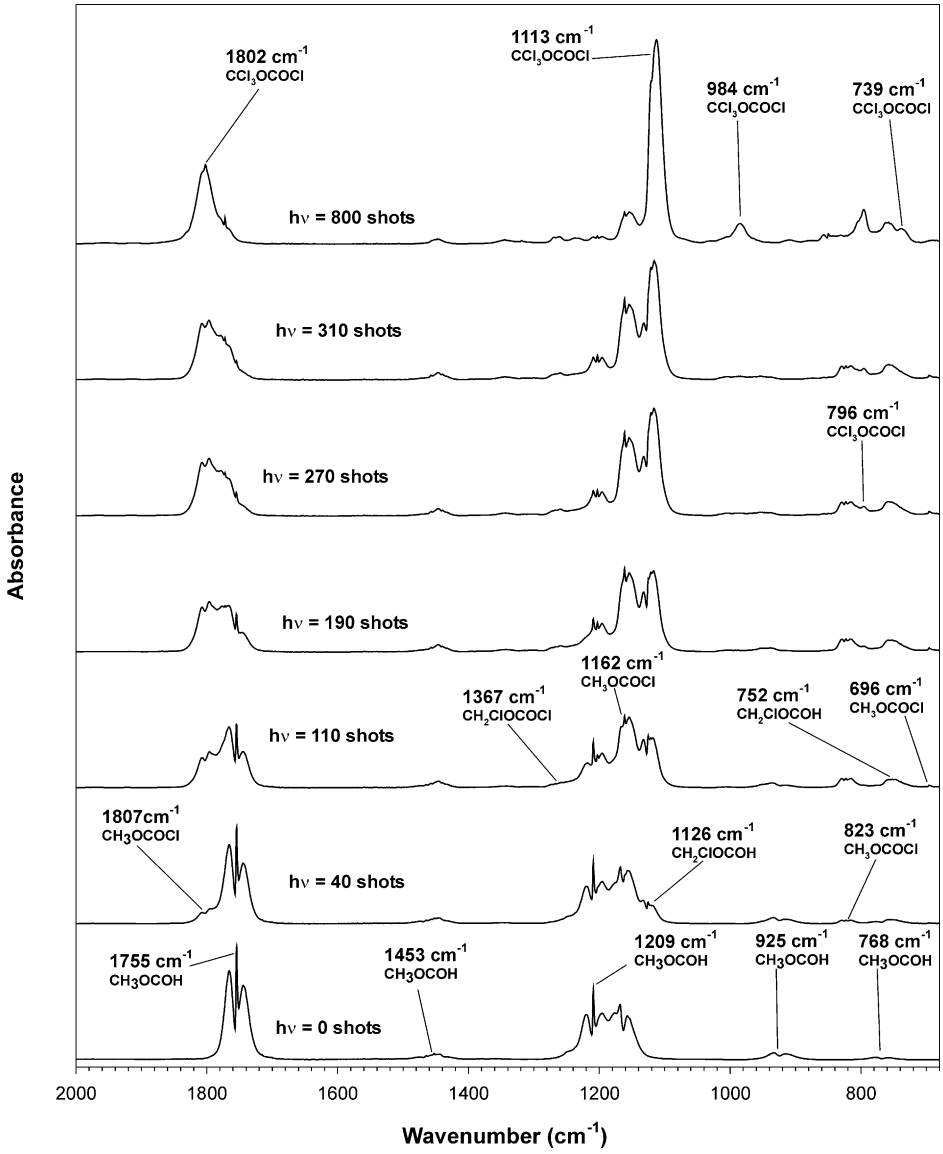

Fig. 1. $CH_3OC(O)H + Cl$ as a function of laser shots (time).

secondary reaction of either $CH_2ClOC(O)H$ or $CH_3OC(O)Cl$ with Cl atoms. Analysis of these spectra shows that <2% of the methyl formate is converted to $CH_2ClOC(O)Cl$. The reaction mechanism for producing $CHCl_2OC(O)Cl$ and $CCl_3OC(O)Cl$ dictates that even smaller amounts of these multiply chlorinated methyl formate species will be produced on the same time scale as production of the singly chlorinated compounds.

At the short time conditions chosen for the determination of the branching ratio, each IR spectrum represents a mixture of $CH_3OC(O)H$, $CH_3OC(O)Cl$, and $CH_2ClOC(O)H$. Measurement of the amount of methyl formate removed versus the amount of $CH_3OC(O)Cl$ and $CH_2ClOC(O)H$ produced allows a determination of the branching ratio. The amount of methyl formate and subsequent chlorinated methyl formate species generated after a given number of laser shots is determined by use of a spectral fitting routine. The observed IR spectra can be described via a linear combination of Beer's Law,

$$A_{\text{total}} = \sum \beta_x \times A_x. \qquad \text{(Equation(I))}$$

Here A_{total} is the measured IR absorbance spectrum, A_x are the IR reference spectra of the components at a specified concentration, β_x indicates the component concentrations and $x = CH_3OC(O)H$, $CH_3OC(O)Cl$, $CH_2ClOC(O)H$, and $CH_2ClOC(O)Cl$ represents the components. The product of $\beta_x \times A_x$ then describes the contribution of a particular species in the gas mixture to the total

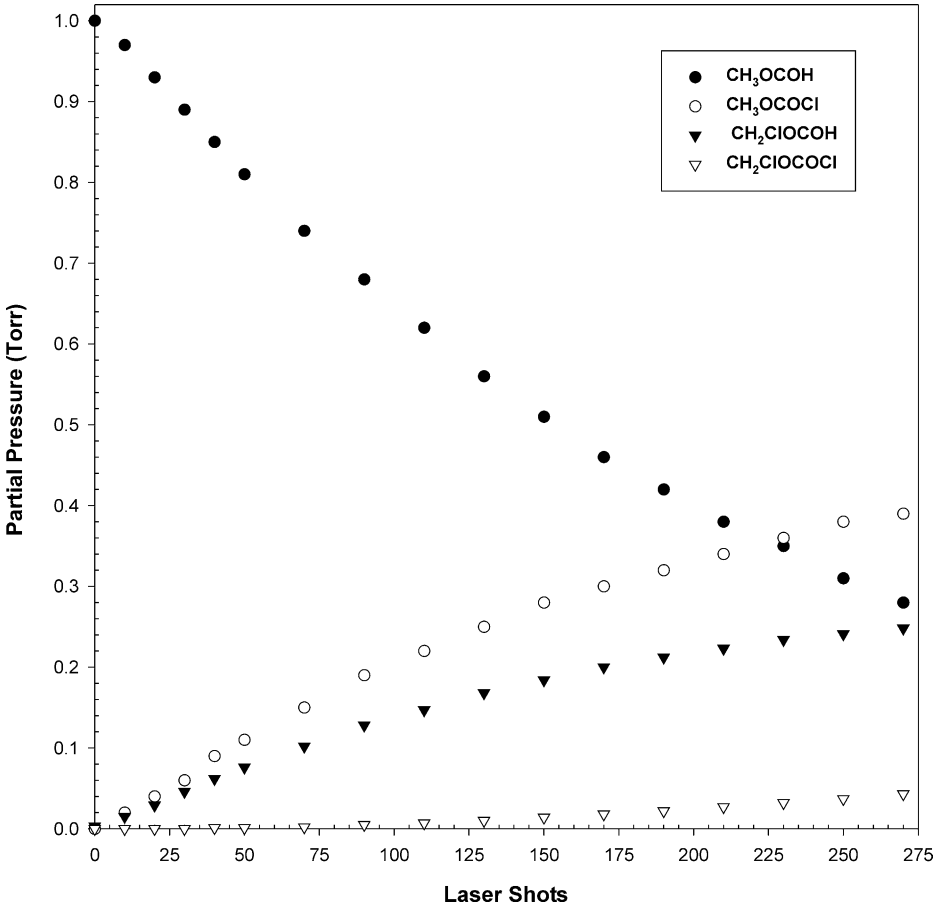

Fig. 2. $CH_3OC(O)H + Cl$ reaction products as a function of laser shots (time).

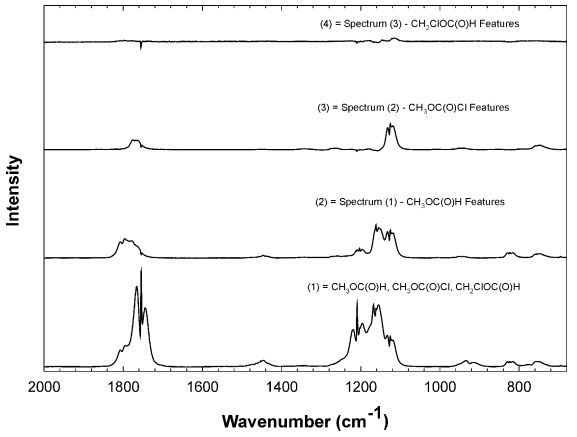

Fig. 3. Spectrum (1): IR spectrum of $CH_3OC(O)H/Cl_2$ mixture after 50 pulses of *hν*. Spectrum (2): Spectral features that remain after subtraction of the IR features indicative of $CH_2OC(O)H$. Spectrum (3): Spectral features that remain after subtraction of the IR features indicative of $CH_3OC(O)Cl$ from Spectrum (2). Spectrum (4): Remaining spectral features after subtraction of $CH_2ClOC(O)H$'s features from Spectrum (3).

absorbance. Using Equation (I) to fit the spectra taken at early photolysis times and solving for $\beta_{CH_3OC(O)H}$, $\beta_{CH_3OC(O)Cl}$, $\beta_{CH_2ClOC(O)H}$, and $\beta_{CH_2ClOC(O)Cl}$ yields the concentration of each species in the gas mixture.

Commercially available samples of $CH_3OC(O)H$ and $CH_3OC(O)Cl$ were used to generate reference spectra for these two species. $CH_2ClOC(O)H$ and $CH_2ClOC(O)Cl$ are not commercially available and the reference spectra were generated by spectral subtraction. In order to generate a clean spectrum of $CH_2ClOC(O)Cl$, a mixture of $CH_3OC(O)Cl$ and Cl_2 was photolyzed with 30 shots of 351 nm photons. The resulting gas mixture is a combination of $CH_3OC(O)Cl$ and $CH_2ClOC(O)Cl$. The IR spectrum of this mixture was measured and all the spectral features indicative of $CH_3OC(O)Cl$ were subtracted. The resulting spectrum represents only $CH_2ClOC(O)Cl$. A similar approach was used for the generation of the $CH_2ClOC(O)H$ reference spectrum. A mixture of $CH_3OC(O)H$ and Cl_2 was photolyzed with 30 shots of 351 nm photons. In this case the resulting mixture is a combination of $CH_3OC(O)H$, $CH_3OC(O)Cl$ and $CH_2ClOC(O)H$. All of the spectral features representing $CH_3OC(O)H$ and $CH_3OC(O)Cl$ were subtracted leaving a clean spectrum of $CH_2ClOC(O)H$.

Fig. 2 depicts the loss of methyl formate and subsequent generation of chlorinated methyl formate species as a function of the number of photolysis pulses (equivalently, time). Fig. 2 shows that for shorter times, mono-chlorinated methyl formate species are produced (i.e., $CH_3OC(O)Cl$ and $CH_2ClOC(O)H$) proportionally to the decrease in methyl formate. As time increases this is followed by the conversion of $CH_3OC(O)Cl$ and $CH_2ClOC(O)H$ to $CH_2ClOC(O)Cl$. No evidence was found for interferences, such as the unimolecular decomposition of $CH_3OC(O)$ or $CH_2OC(O)H$, the decomposition of the reaction products due to the photolysis laser flash or possible heterogeneous reactions. Spectrum (1) in Fig. 3 is the IR spectrum of a methyl formate/Cl_2 gas mixture that has been photolyzed for 50 pulses. Spectrum (2) in Fig. 3 shows the resulting spectrum after all the features due to $CH_3OC(O)H$ have been subtracted from Spectrum (1). Spectrum (3) in Fig. 3, is the result of the subtraction of all the spectral features indicative of $CH_3OC(O)Cl$ from Spectrum (2). Spectrum (4) shows the results from the subtraction of all the spectral features of $CH_2ClOC(O)H$ from Spectrum (3), the resulting spectrum is void of any spectral features. The absence of any spectral features in Spectrum (4) verifies that the reactions (2)–(5) are responsible for the observed decay of methyl formate in the conditions used in this study.

Table 1 summarizes the results for the calculation of the branching ratio for each trial. The branching ratio shows no pressure dependence within the 20–200 Torr range of the experiments. The carbonyl hydrogen of $CH_3OC(O)H$ is found to be extracted 58% of the time and correspondingly, the methyl hydrogen 42% of the time. Wallington et al.'s [16] recent work describing the degradation pathway of methyl formate yields a branching ratio of $(55 \pm 7)\%$, which compares favorably with the present result.

The uncertainty in the measured branching ratio is calculated to be $\pm 6\%$. Factors contributing to the uncertainty include a 4% error in the determination of the reference spectra. This is due to the uncertainty of the reference gas pressure and

Table 1
Branching ratio for the $Cl + CH_3OC(O)H$ reaction

Branching ratio analysis					
Trial no.	$CH_3OC(O)H$ (Torr)	Cl_2 (Torr)	Buffer (Torr)	% Carbonyl hydrogen extraction	% Methyl hydrogen extraction
1	2.3	24.7	0	56.8	43.2
2				56.5	43.5
3				55.7	44.3
1	1	20.4	0	57.7	42.3
2				58.8	41.2
3				58.2	41.8
1	3.1	20.7	0	58.7	41.3
2				57.5	42.5
3				56.1	43.9
1	1.1	21.1	0	55.4	44.6
2				55.5	44.5
1	2.1	20	21.3	60.4	39.6
2				58.3	41.7
3				60.9	39.1
1	2	21	21	56.7	43.3
2				56.4	43.6
3				56	44
1	2.1	20.4	53.4	60.6	39.4
2				59.8	40.2
3				59	41
1	2.4	21.5	51.3	56.8	43.2
2				56.5	43.5
3				56.1	43.9
4				55.9	44.1
1	2.1	20.2	103.9	58.3	41.7
2				58.4	41.6
3				58.7	41.3
1	2.1	21.8	210.3	62	38
2				61	39
3				60.5	39.5
			Average =	58.0	42.0

baseline drift in the spectrometer. In addition to the error in the reference spectra, the error associated with the fitting routine and hence calculation of the coefficients (β_x) is considered. Error in the determination of the coefficients for methyl formate never exceeded 0.05% for any of the fitted spectra used for the branching ratio and represents 2σ from the fit. Similarly, error in the determination of the coefficients for both $CH_3OC(O)Cl$ and $CH_2ClOC(O)H$ never exceeded 1% and 2.5% respectively.

Fundamental to this study and the subsequent data analysis was the necessity of generating reference spectra for $CH_3OC(O)Cl$, $CH_2ClOC(O)H$, and $CH_2ClOC(O)Cl$ that are free of impurities. Spectral subtraction from a composite spectrum containing IR features indicative of $CH_3OC(O)H$, $CH_3OC(O)Cl$, and $CH_2ClOC(O)H$ was used to

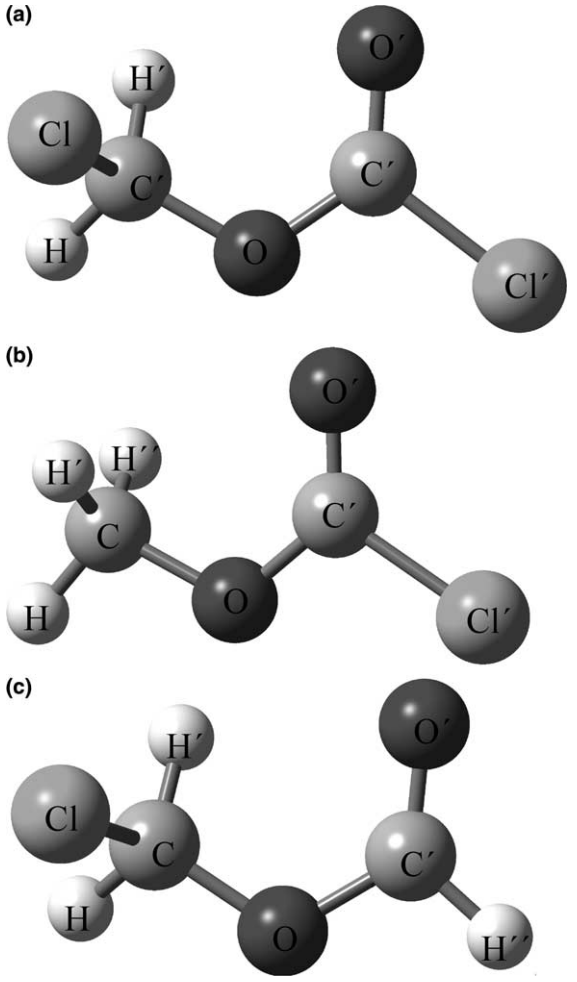

Fig. 4. (a) Structure of $CH_2ClOC(O)Cl$; (b) structure of $CH_3OC(O)Cl$; (c) structure of $CH_2ClOC(O)H$.

obtain the IR spectrum of $CH_2ClOC(O)H$. In a similar manner, spectral subtraction was also utilized to generate an IR spectrum of $CH_2ClOC(O)Cl$. Ab initio calculations were used to simulate the IR spectrum of $CH_2ClOC(O)H$ and $CH_2ClOC(O)Cl$. This was done in order to verify that the IR spectrum obtained by spectral subtraction contained only features indicative of $CH_2ClOC(O)H$ and $CH_2ClOC(O)Cl$. $CH_3OC(O)Cl$ is available commercially, as such, the calculated IR spectrum when compared to the experimental spectrum serves as a calibrant.

Fig. 4a–c depict the optimized geometry found at the B3LYP/6-311++G(3df,3pd) level for $CH_2ClOC(O)Cl$, $CH_3OC(O)Cl$, and $CH_2ClOC(O)H$, respectively. Table 2 gives the bond lengths, angles, and dihedrals. Table 3 presents a comparison of the calculated fundamental frequencies and the analogous experimental features. Included in this table is a qualitative description for the predicted and experimentally determined strength of each IR feature. Analysis of the predicted strengths compared to the experimentally determined value shows good qualitative agreement throughout the spectral region.

Fig. 5 superimposes the calculated and scaled IR spectrum on the experimentally measured spectra for $CH_2ClOC(O)Cl$, $CH_3OC(O)Cl$, and $CH_2ClOC(O)H$. Fig. 5 shows excellent agreement between the calculated and experimental IR features. For example, one of the prominent features found in each experimental spectrum is the carbonyl stretch. These occur at 1803, 1796, and 1770 cm^{-1} for $CH_2ClOC(O)Cl$, $CH_3OC(O)Cl$, and $CH_2ClOC(O)H$, respectively. The corresponding calculated features are predicted to occur at 1811, 1805, and 1776 cm^{-1} for $CH_2ClOC(O)Cl$, $CH_3OC(O)Cl$, and $CH_2ClOC(O)H$, respectively. The differences between the experimental and calculated values are 8, 9, and 6 cm^{-1}. The strongest feature in each IR spectrum in Fig. 5 is the C′–O stretch. Comparison of the calculated to the experimental IR spectrum in all three species shows excellent agreement, with a difference of only 19, 20, and 7 cm^{-1} for $CH_2ClOC(O)Cl$, $CH_3OC(O)Cl$, and $CH_2ClOC(O)H$, respectively. The excellent agreement between the experimentally and calculated IR spectra suggest that the lowest energy structure for all three species has been identified as well as indicating that the reference spectra used for the analysis of the branching ratio of methyl formate contain only features indicative of $CH_2ClOC(O)Cl$, $CH_3OC(O)Cl$, and $CH_2ClOC(O)H$.

4. Discussion

Atomic chlorine has been measured to extract the carbonyl hydrogen and methyl hydrogen 58% and 42% (±6%) of the time, respectively. The previous computational work by Good et al. [11]

Table 2
Minimum energy sturctures for $CH_2ClOC(O)Cl$, $CH_3OC(O)Cl$, and $CH_2ClOC(O)H$

	B3LYP/				
	6-31G(d)	6-31G(d,p)	6-311++G(d,p)	6-311++G(2df,2p)	6-311++G(3df,3pd)
$CH_2ClOC(O)Cl$[a]					
C′–Cl′	1.766	1.766	1.762	1.757	1.754
O–C′	1.348	1.345	1.345	1.343	1.344
C–O	1.422	1.422	1.422	1.420	1.421
Cl–C	1.798	1.799	1.797	1.791	1.787
C′–O′	1.192	1.192	1.186	1.184	1.187
H–C	1.087	1.087	1.084	1.082	1.084
H′–C	1.088	1.088	1.086	1.084	1.086
O–C′–Cl′	108.3	108.3	108.5	108.5	108.4
C–O–C′	115.6	115.6	116.2	116.3	115.9
Cl–C–O	111.5	111.4	111.4	111.4	111.4
O′–C′–Cl′	124.2	124.2	124.0	124.1	124.1
H′–C–O	110.9	110.9	111.0	111.0	110.9
H–C–O	105.7	105.8	105.8	105.9	105.8
C–O–C′–Cl′	178.5	178.4	178.2	178.5	178.4
Cl–C–O–C′	−87.6	−87.9	−88.0	−87.7	−86.3
O′–C′–O–C	−2.3	−2.4	−2.5	−2.2	−2.3
H′–C–O–C′	32.6	32.1	32.0	32.3	33.8
H–C–O–C′	155.4	155.1	155.3	155.4	156.8
CH_3OCOCl[a]					
C′–Cl′	1.780	1.779	1.775	1.769	1.765
C′–O	1.329	1.329	1.326	1.324	1.324
O–C	1.448	1.449	1.451	1.447	1.446
C–H	1.089	1.089	1.090	1.084	1.084
C′–O′	1.195	1.195	1.190	1.188	1.188
C–H′	1.092	1.092	1.090	1.087	1.087
C–H″	1.092	1.092	1.090	1.087	1.087
O–C′–Cl′	108.6	108.6	108.8	108.8	108.9
C–O–C′	114.4	114.3	115.1	115.1	115.1
H–C–O	104.9	105.0	104.9	105.0	105.0
O′–C′–Cl′	123.4	123.4	123.1	123.3	123.3
H′–C–O	110.1	110.2	110.0	110.0	110.0
H″–C–O	110.1	110.2	110.0	110.1	110.1
C–O–C′–Cl′	180.0	180.0	180.0	−180.0	−180.0
H–C–O–C′	180.0	180.0	180.0	180.0	180.0
O′–C′–O–C	0.0	0.0	0.0	0.0	0.0
H′–C–O–C′	−60.6	−60.5	−60.7	−60.5	−60.6
H″–C–O–C′	60.6	60.5	60.6	60.5	60.5
$CH_2ClOCOH$[a]					
C′–H″	1.099	1.099	1.097	1.095	1.095
C′–O	1.362	1.363	1.361	1.357	1.356
O–C	1.411	1.411	1.412	1.410	1.410
Cl–C	1.808	1.808	1.806	1.800	1.795
C′–O′	1.201	1.201	1.195	1.193	1.192
H–C	1.088	1.088	1.086	1.084	1.084
C–H′	1.087	1.087	1.084	1.082	1.082
O–C′–H″	108.2	108.3	108.3	108.4	108.5
C–O–C′	116.5	116.4	117.2	117.2	117.1
Cl–C–O	111.3	111.3	111.3	111.3	111.3
O′–C′–H″	125.8	125.9	125.9	125.7	125.7

Table 2 (*continued*)

	B3LYP/				
	6-31G(d)	6-31G(d,p)	6-311++G(d,p)	6-311++G(2df,2p)	6-311++G(3df,3pd)
H–C–O	111.1	111.2	111.3	111.3	111.2
H′–C–O	106.8	106.9	106.8	106.9	106.8
C–O–C′–H″	178.8	178.7	178.7	178.9	178.9
Cl–C–O–C′	−91.1	−91.4	−90.6	−90.6	−90.2
O′–C′–O–C	−1.9	−1.9	−1.9	−1.7	−1.7
H–C–O–C′	28.4	27.9	28.8	28.9	29.3
H′–C–O–C′	152.1	151.8	152.8	152.7	153.0

[a] Bond lengths are reported in angstroms, angles and dihedrals in degrees. All calculation done using the B3LYP level of theory.

Table 3
Experimental verse Calculated IR frequencies for $CH_2ClOC(O)Cl$, $CH_3OC(O)Cl$, and $CH_2ClOC(O)H$

Vibrational mode	Frequencies (cm^{-1})	Intensity		
	Calculated (B3LYP/6-31G(d) level)[a]	Experimental	Calculated (KM/mole)	Experimental
$CH_3OC(O)Cl$				
1	3078	3016	8.1	Weak
2	3046	2969	9	Weak
3	2967	2854	17.5	Weak
4	1805	1796	526.1	Strong
5	1461	1457	12.9	Weak
6	1455	1447	28.3	Weak
7	1432	1439	5.1	Weak
8	1183	1203	193.7	Medium
9	1142	NA	0.7	
10	1136	1162	137.4	Strong
11	946	823	228.6	Medium
12	797	696	14.5	Weak
13	662	NA	72.5	
14	453	NA	9	
15	384	NA	11.9	
16	255	NA	2.5	
17	159	NA	0.4	
18	116	NA	1.5	
$CH_2ClOC(O)Cl$				
1	3106	NA	0	
2	3026	2998	6.9	Weak
3	1811	1803	504.9	Medium
4	1438	1458	15.3	Weak
5	1339	1357	21.1	Weak
6	1252	1270	48	Medium
7	1096	1115	393.6	Strong
8	988	1003	148.5	Weak
9	966	801	88.2	Medium
10	777	764	79.5	Medium
11	711	685	31.2	Weak
12	650	NA	89	
13	469	NA	12.7	
14	438	NA	5.4	
15	310	NA	1.2	

Table 3 (*continued*)

Vibrational mode	Frequencies (cm^{-1})	Intensity		
	Calculated (B3LYP/6-31G(d) level)[a]	Experimental	Calculated (KM/mole)	Experimental
16	264	NA	3.3	
17	81	NA	0.7	
18	61	NA	1.7	
$CH_2ClOC(O)H$				
1	3101	NA	1.3	
2	3024	2998	12.9	Weak
3	2978	2953	50.6	Medium
4	1776	1770	246.6	Strong
5	1439	1450	9.4	Weak
6	1360	NA	1.1	
7	1338	1343	32.4	Weak
8	1254	1267	28.1	Weak
9	1112	1125	455.9	Strong
10	995	1119	1.7	Strong
11	989	1008	5.8	Weak
12	932	947	34.7	Weak
13	721	752	9.1	Medium
14	701	NA	120.1	
15	409	NA	16.6	
16	309	NA	13.3	
17	223	NA	9.8	
18	65	NA	1.9	

[a] Scaled by 0.9614.

predicted 90% probability for extraction of the carbonyl hydrogen, but with a range of 65–97%. The inconsistency between the two results is thought to arise from the large relative uncertainties in the calculated activation barriers as well as in the determination of the calculated vibrational frequencies. The IR spectrum of $CH_2ClOC(O)H$ and $CH_2OC(O)Cl$, two compounds unavailable commercially, has been measured experimentally and compared to calculated IR spectrum generated using high level ab initio calculations. Excellent agreement was found between the experimental and the calculated spectrum.

In addition to the insight gained about the distribution of methyl formate oxidation products, the branching ratio allows determinations of the individual rate constants for hydrogen extraction by atomic chlorine. Three separate groups have reported the overall $Cl + CH_3OC(O)H$ rate constant. Wallington et al. [17], using a relative rate technique reported the rate constant at 298 K to be $(1.4 \pm 0.1) \times 10^{-12}$ cm^3 mol^{-1} s^{-1}. Notario et al. [18], used a pulsed laser photolysis–resonance fluorescence technique and reported a value of $(1.8 \pm 0.2) \times 10^{-12}$ cm^3 mol^{-1} s^{-1}. In addition, Good et al. [11], using the relative rate technique as well, reported a value of $(1.4 \pm 0.5) \times 10^{-12}$ cm^3 mol^{-1} s^{-1}. Combining the overall rate constant with the branching ratio results and propagating the 6% uncertainty with the 36% uncertainty in the rate constant reported by Good et al. [11], leads to the individual hydrogen extraction rate constants for the methyl formate and chlorine reaction:

$$k_{1a} = (8.1 \pm 2.9) \times 10^{-13} \text{ cm}^3 \text{ mol}^{-1} \text{ s}^{-1}$$

$$k_{1b} = (5.9 \pm 2.1) \times 10^{-13} \text{ cm}^3 \text{ mol}^{-1} \text{ s}^{-1}$$

5. Conclusions

The branching ratio for extraction of a hydrogen from methyl formate by chorine atoms has been determined. The branching ratio was found to

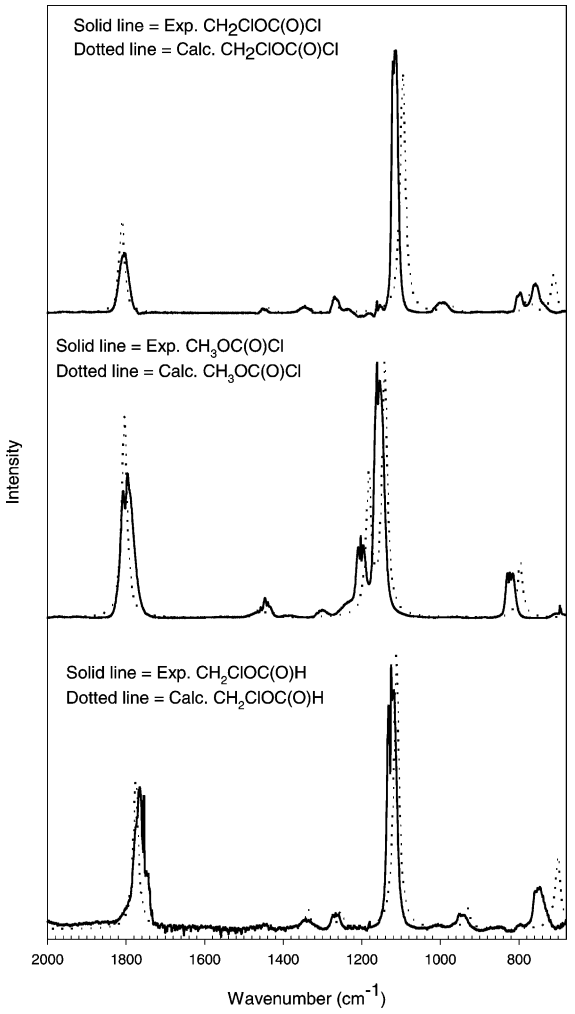

Fig. 5. Calculated vs. experimental IR spectrum for chlorinated methyl formate species.

be 58/42% (±6%) for extraction of the carbonyl hydrogen and a methyl hydrogen, respectively. High level ab initio calculations were used to calculated the lowest energy structures of $CH_3OC(O)Cl$, $CH_2ClOC(O)H$, and $CH_2ClOC(O)Cl$. Ab initio calculations were also used to verify the experimentally detemermined IR spectra of $CH_3OC(O)Cl$, $CH_2ClOC(O)H$, and $CH_2ClO(O)Cl$. Excellent agreement was found between the experimental and calculated IR spectra. The branching ratio for hydrogen extraction from methyl formate by chlorine atoms in conjunction with the overall $Cl + CH_3OC(O)H$ rate reaction rate constant was used to determine the individual hydrogen extraction rate constants ($k_{1a} = 8.1 \times 10^{-13}$ cm^3 mol^{-1} s^{-1}, $k_{1b} = 5.9 \times 10^{-13}$ cm^3 mol^{-1} s^{-1}).

References

[1] A.M. Rouhi, Chem. Eng. News 44 (1985) 37.
[2] S.M. Japar, T.J. Wallington, J.F.O. Richert, J.C. Ball, Int. J. Chem. Kinet. 22 (1990) 1257.
[3] M.E. Jenkin, G.D. Hayman, T.J. Wallington, M.D. Hurley, J.C. Ball, O.J. Nielsen, T. Ellerman, J. Phys. Chem. 97 (1993) 11712.
[4] T.J. Wallington, M.D. Hurley, J.C. Ball, M.E. Jenkin, Chem. Phys. Lett. 211 (1993) 41.
[5] S. Langer, E. Ljungstrom, T. Ellerman, O.J. Nielsen, J. Sehested, J. Chem. Phys. Lett. 240 (1995) 53.
[6] J. Sehested, T. Mogelberg, T.J. Wallington, E.W. Kaiser, O.J. Nielsen, J. Phys. Chem. 100 (1996) 17218.
[7] J. Sehested, K. Sehested, J. Platz, H. Egsgaard, O.J. Nielsen, Int. J. Chem. Kinet. 29 (1997) 627.
[8] M.M. Maricq, J.J. Szente, J.D. Hybl, J. Phys. Chem. 101 (1997) 5155.
[9] L. Zhuangjie, G. Jeong, J.S. Francisco, J. Hansen, D.A. Good, J. Phys. Chem. 103 (1999) 10893.
[10] D.A. Good, J.S. Francisco, J. Phys. Chem. 104 (2000) 1171.
[11] D.A. Good, J.S. Francisco, J. Hansen, M. Kamboures, R. Santiono, J. Phys. Chem. 104 (2000) 1505.
[12] M. Bartels, K. Hoyermann, U. Lange, Ber. Bunsenges. Phys. Chem. 93 (1989) 423.
[13] M.J. Frisch et al., GAUSSIAN 98, Revision A.7, Gaussian, Inc., Pittsburgh, PA, 1998.
[14] A.P. Scott, L. Radom, J. Phys. Chem. 100 (1996) 16502.
[15] D.A. Good, M. Kamboures, R. Santiano, J.S. Francisco, J. Phys. Chem. A. 103 (1999) 9230.
[16] T.J. Wallington, M.D. Hurley, T. Maurer, I. Barnes, K.H. Becker, G.S. Tyndall, J.J. Orlando, A.S. Pimentel, M. Bilde, J. Phys. Chem. 105 (2001) 5146.
[17] T.J. Wallington, M.D. Hurley, J.C. Ball, M.E. Jenkin, Chem. Phys. Lett. 211 (1993) 41.
[18] A. Notario, G. Le Bras, A. Mellouki, J. Phys. Chem. 102 (1998) 3112.